



Thermal degradation process of the cured phenolic triazine thermoset resin (Primaset[®] PT-30). Part I. Systematic non-isothermal kinetic analysis

Bojan Janković*

Department of Dynamics and Matters Structure, Faculty of Physical Chemistry, University of Belgrade, Studentski trg 12-16, P.O. Box 137, 11001 Belgrade, Serbia

ARTICLE INFO

Article history:

Received 30 December 2010
Received in revised form 8 March 2011
Accepted 16 March 2011
Available online 31 March 2011

Keywords:

Thermal degradation
Primaset[®] PT-30
Systematic kinetic analysis
Predictions
Lifetime

ABSTRACT

The non-isothermal degradation of the cured Primaset[®] PT-30 resin in nitrogen atmosphere was examined. It was found that the total mass loss of the sample strongly depends on the heating rate. Using different kinetic methods, the complete kinetic triplet of investigated process was performed. It was found that process can be successfully described by the following kinetic triplet: $E_a = 193.8 \text{ kJ mol}^{-1}$, $A = 9.82 \times 10^{10} \text{ min}^{-1}$ and $f(\alpha) = (1 - \alpha)^{3/2}$. Also, it was found that with single step reaction model (Fn-type) with $n = 3/2$, a complex and multi-step degradation process can be successfully approximated. Isothermal predictions of degradation were carried out at temperatures 400 °C, 420 °C and 450 °C. The observed disagreement between the prediction curves and experimental curves in terms of degradation lifetime at corresponding temperatures could lay in a very strong dependence of reaction system on the heating rate, which means on the temperature of degradation. It was concluded that due to high thermal resistance, Primaset[®] PT-30 resin needs more temperature to process it to produce parts for usage. The lifetime parameters indicate that the service/process temperature has a strong influence on the degradation process of the cured Primaset[®] PT-30 resin.

© 2011 Elsevier B.V. All rights reserved.

1. Introduction

Phenolic triazine (PT) precursor resin is a reaction product of novolac resin and cyanogen halide. Phenolic triazine network is formed by the thermal cyclotrimerization of the cyanate ester of novolac [1,2]. Synthesis procedure of PT resin can be conducted as the novolac hydroxyl groups reacted with cyanogens bromide under basic conditions to produce cyanate ester resins [2,3]. Cyanate esters can thermally crosslink to form void free networks, wherein at least some triazine rings form. The resultant networks possess high T_g s (glass transition temperature), high char yield at 900 °C and high decomposition temperatures [2].

It is an ideal matrix system for composites, because it combines the processibility convenience of epoxies and the thermal capabilities of poly-imides and fire resistance of phenolics. The absence of volatile by-products during cure renders them attractive matrices for void-free moldings and composites.

PT resin offers considerable processing flexibility since their consistency ranges from low viscous liquids to semi solids, with gel temperatures that can be tuned by catalysis using a host of materials. PT resins possess better thermo-oxidative stability and char-yield than conventional phenolics, because they are mostly cross-linked by triazine groups. The proximity of the hydroxyl

groups in phenolic resin renders these methylene bridges thermo-oxidatively fragile, and the decomposition process is accelerated by the number of dihydroxy phenyl methylene groups [4]. It is stated that there is always a thermo-oxidative process during degradation irrespective of the atmosphere. The high oxygen content of phenol is also responsible for this. The degradation mechanism of phenolic resins was suggested by Conley [5]. PT resins, on the other hand, are cross-linked mostly by triazine phenyl ether linkages, which confer both thermo-oxidative stability and toughness to the system. The evidence for better thermo-oxidative stability is obtained from the thermal behavior of the systems in both air and the inert atmosphere [6,7]. The essentially super imposable thermograms point towards a non-oxidative mechanism of degradation for PT systems. This implies better prospects for application of this type of resin for thermo-structural uses in aerospace in place of conventional phenolics. Laser ablation studies on a series of ablatives including PT resin have confirmed their potentiality for such applications [8]. Ablative formulations for rocket nozzle applications contain PT resin as one of the components [9]. The PT resin systems have been successfully employed in filament winding of cylindrical structures such as pressure bottles which retain 83% of their room temperature properties at 288 °C [10].

Despite many claims about the superiority of PT systems over other cyanates and phenolics, there are only a few reports on its commercial utilization. One reason for this is that the resin generally shows inconsistency in cure behavior due to catalysis by the spurious impurities adsorbed on the polymer during its

* Tel.: +381 11 2187 133; fax: +381 11 2187 133.
E-mail address: bojanjan@ffh.bg.ac.rs

synthesis. It is not easy to purify the polymer scrupulously, to the level of monomeric dicyanates. Absorbed moisture can also cause variations in cure behavior. Unpredictable cure profiles impose processing difficulties and large property variations. It is generally found that the synthesized resins exhibit poor shelf life, particularly when the precursor novolac possesses higher molar mass. PT resins, structurally modified with both rigid and flexible groups in their backbone were not helpful in improving either shelf life or thermal stability. Thus, a flexible pentadecenyl group (i.e. cardanol) was introduced through copolymerization of phenol with cardanol, and subsequently using the modified novolac for cyanation. The thermal stability decreased proportional to the cardanol content and the resins exhibited poorer shelf-life [11]. PT resin is commercially available under the trade name Primaset® PT-15, PT-30, PT-60 and PT-90, which essentially differ in their molar masses [12]. The gel time can be tuned by catalyst concentration. The generally recommended catalysts are zinc octoate/nonyl phenol, cobalt naphthenate, copper salts etc.

Thermoanalytical techniques (such as thermogravimetric analysis (TGA), differential thermal analysis (DTA) or differential scanning calorimetry (DSC)) are valuable tools for the characterization of thermosetting polymers [13]. Thermal techniques are essential to the study of degradation processes of thermosetting resins under different reaction atmospheres [13,14].

The primary goal of this paper was to perform the systematic kinetic analysis of degradation process of the cured phenolic triazine resin commercially known as Primaset® PT-30. In the first part of a comprehensive study of this system, the kinetic analysis of non-isothermal degradation process under nitrogen atmosphere was carried out. By the literature survey, author did not find the results associated with the real derivative values of 'kinetic triplet' (the apparent activation energy (E_a), the pre-exponential factor (A) and the function of reaction mechanism $f(\alpha)$; [E_a , A , $f(\alpha)$]), for Primaset® PT-30 degradation process under dynamic conditions. Kinetic characterization of thermoset resins is fundamental in understanding the structure–property–processing relationship for high performance composite processing and application. However, thermal stability and combustibility of Primaset® PT-30 resin was recently investigated by several researchers [15–18].

The corresponding 'isothermal predictions' of the investigated process, derived from the results of non-isothermal kinetic study, are also presented in this paper. This approach is important from a practical standpoint, in order to predict the thermal behavior of the tested system in different experimental conditions.

2. Experimental

2.1. Materials and methods

Primaset® PT-30 cyanate ester (Oligo(3-methylene-1,5-phenylenecyanate)) (manufactured by Lonza Chemical Corporation Ltd. (Lonza Cologne AG, 50829 Cologne, Germany)) (Molecular mass, $M = 381.39 \text{ g mol}^{-1}$) in this study was one-part, pure solid, commercial sample, which was used as received without further purification and catalysts.

Primaset® PT-30 is a thermoset resin, with 65% char yield (same as phenolics), less than 0.5% volatiles, no gaseous by-products during cure, a low viscosity at RTM temperatures (80 c.p.s. at 121 °C) and post-curable [19].

The high purity tri-functional cyanate ester novolac monomer was thermally cured in convection oven without catalyst for 4 h at $T = 250 \text{ °C}$ to more than 95% conversion, in accordance with procedure described elsewhere [17,18]. The fully cured samples were $5 \text{ cm} \times 5 \text{ cm} \times 0.65 \text{ cm}$ solid plaques that were semitransparent.

Curing the cyanate ester novolac monomer produces a tightly cross-linked thermoset network of oxygen-linked triazine rings (called cyanurates) having the repeat unit atomic composition as $\text{C}_8\text{H}_5\text{NO}$. These polycyanurate samples were used directly for thermogravimetric (TG) measurements.

2.2. Thermogravimetric analysis (TGA)

A thermogravimetric analyzer (TA Instruments SDT 2960 device capable for simultaneous TGA–DTA analysis) was used to study the degradation process of cured samples (sample sizes of approximately 5 mg were used for experiments). The TGA cell was purged for 15 min with flowing nitrogen (99.998 vol% purity grades) (with flow rate of $\varphi = 0.10 \text{ L min}^{-1}$) to remove residual air, after which the samples were heated from 25 °C to 800 °C. The non-isothermal scans were performed at selected heating rates (β) in a very wide range of values, ranging from 0.01 to 100 °C min^{-1} ($\beta = 0.01, 0.10, 1, 10$ and 100 °C min^{-1}). A wide range of heating rates is used to a more precise determination of kinetic parameters, and values of the onset degradation temperature (T_i) in accordance with ASTM E698 standard [20].

In order to perform kinetic prediction, the corresponding isothermal measurements were conducted at three different operating temperatures. The same instrument was used to study the isothermal degradation process of cured samples (sample sizes of approximately between 4 and 5 mg were used for experiments) at the following operating temperatures: $T = 400, 420$ and 450 °C . Reaction atmosphere is the same as in the case of non-isothermal scans, with the same carrier gas flow. The samples were heated at a rate of 200 °C min^{-1} from the starting temperature to the temperature of the isothermal degradation. Before operating, the system was stabilized for 1 h. The actual mass losses of the samples at 400, 420 and 450 °C were as follows: $\Delta m_f = 8, 12$ and 15.5% , respectively.

In order to confirm the repeatability and authenticity of the generated data for all considered cases, the experiments were repeated three times at every heating rate and every operating temperature, where the average TG trace among them was used as the representative thermo-analytical curve in the present manuscript. The observed deviations were very little.

3. Theoretical background

In non-isothermal kinetics of heterogeneous condensed phase reactions, it is usually accepted that the reaction rate is given by the following equation [21]:

$$\frac{d\alpha}{dt} = \beta \cdot \frac{d\alpha}{dT} = A \exp\left(\frac{-E_a}{RT}\right) f(\alpha) \quad (1)$$

where α is the degree of conversion ($\alpha = (m_o - m)/(m_o - m_f)$) where m_o , m and m_f are the initial, actual and the final mass of the sample, respectively), T is the absolute temperature, t is the time, $f(\alpha)$ is the differential conversion function (or the analytical function of reaction mechanism), R is the gas constant, β is the linear constant heating rate ($\beta = dT/dt$), A and E_a are the pre-exponential factor and the apparent activation energy given by the Arrhenius equation.

By integrating Eq. (1), the integral rate equation, so-called the temperature integral, can be expressed as:

$$g(\alpha) = \int_0^\alpha [f(\alpha)]^{-1} d\alpha = A\beta^{-1} \int_0^T \exp\left(\frac{-E_a}{RT}\right) dT \quad (2)$$

where $g(\alpha)$ is the integral conversion function. If E_a/RT is replaced by a new variable x and integration limits transformed, Eq. (2) becomes:

$$g(\alpha) = AE_a\beta^{-1}R^{-1} \int_x^\infty \exp(-x)x^{-2} dx = AE_a\beta^{-1}R^{-1}p(x) \quad (3)$$

where $p(x)$ is the exponential integral, which has no analytic solution [22]. However, there are many approximations that make it possible to obtain the kinetic parameters through the linearization of the experimental data [23–27]. There are more complex variations of $p(x)$, such as those put forward by Senum and Yang [28] and Agrawal [29] whose approximations of the temperature integral at an interval of x offer far higher accuracy and lower error.

3.1. Isoconversional methods

Isoconversional approach in non-isothermal experiments assumes that for a given degree of conversion, the reaction mechanism does not depend on the heating rate.

By applying logarithms to Eq. (1), the differential isoconversional method suggested by Friedman (FR) [30] is obtained:

$$\ln \left[\beta \left(\frac{d\alpha}{dT} \right) \right] = \ln[Af(\alpha)] - \frac{E_a}{RT} \quad (4)$$

The linear plot of $\ln[\beta(d\alpha/dT)]$ versus $1/T$, obtained from DTG curves recorded for several heating rates makes it possible to determine E_a and the kinetic parameter $\ln[Af(\alpha)]$, for every value of α .

By using the Coats–Redfern [31] approximation to solve Eq. (3) and considering that $2RT/E_a$ is much lower than unity, the Kissinger–Akahira–Sunose (KAS) [25,26] equation can be written in the form:

$$\ln \left(\frac{\beta}{T^2} \right) = \ln \left[\frac{AR}{g(\alpha)E_a} \right] - \frac{E_a}{RT} \quad (5)$$

For each degree of conversion, the linear plot of $\ln(\beta/T^2)$ versus $1/T$ enables E_a and $\ln[AR/g(\alpha)E_a]$ to be determined from the slope and the intercept, respectively. If the reaction model, $g(\alpha)$, is known, the corresponding pre-exponential factor can be calculated for each conversion.

If E_a does not vary with α , the study is straightforward and one single kinetic triplet describes the degradation process. If E_a changes with α , the process is more complex and the shape of E_a – α curve may provide the information on the reaction mechanism [32]. Due to the compensatory effect, it is also necessary to study the evolution of the second kinetic parameter, which includes the pre-exponential factor and the reaction model. Not using this second parameter could lead to errors.

3.2. Coats–Redfern method

The Coats–Redfern (CR) [31] method is based on Eq. (5) in the following form:

$$\ln \left[\frac{g(\alpha)}{T^2} \right] = \ln \left(\frac{AR}{\beta E_a} \right) - \frac{E_a}{RT} \quad (6)$$

For a given model and heating rate, the linear plot of the left-hand side of Eq. (6) versus $1/T$ allowed us to obtain the average apparent activation energy and average pre-exponential factor from the slope and the intercept. Then, we can choose the reaction model with the apparent activation energy similar to that obtained isoconversionally and with a good linear correlation coefficient.

3.3. Composite kinetic methods

The composite kinetic methods pre-suppose one single set of kinetic parameters for all conversions and heating rates. In this way, all experimental data can be superimposed in one single master curve.

Composite integral method I [33,34] is based on the CR equation, which is re-written as follows:

$$\ln[\beta g(\alpha)T^{-2}] = \ln \left(\frac{AR}{E_a} \right) - \frac{E_a}{RT} \quad (7)$$

For each form of $g(\alpha)$, the curve $\ln[\beta g(\alpha)T^{-2}]$ versus T^{-1} was plotted for the experimental data obtained at the different heating rates. Then, we can choose the reaction model for which the data falls in a single master straight line and which gives the best linear correlation coefficient. A single set of kinetic parameters, E_a and A , can be obtained from the slope and the intercept of the straight line, respectively. The obtained values of kinetic parameters must be similar to those obtained for each heating rate using the CR method.

Composite differential method I [35] is based directly on Eq. (4). In that case, Eq. (4) can be re-written in the following form:

$$\ln \left[\frac{\beta(d\alpha/dT)}{f(\alpha)} \right] = \ln(A) - \frac{E_a}{RT} \quad (8)$$

The data for different heating rates must be grouped together in a single master straight line, from which a single set of kinetic parameters (E_a and A) is obtained.

3.4. Compensation effect (isokinetic relationship (IKR))

The apparent activation energy and the pre-exponential factor can be linked due to a compensation effect or the isokinetic relationship (IKR) through the following equation [36,37]:

$$\ln A_{\xi} = a + bE_{a,\xi} \quad (9)$$

where a and b are the compensation constants and the subscript ξ refers to a factor producing a change in the kinetic parameters (conversion, heating rate and model).

The slope $b = 1/RT_{iso}$ is related to the isokinetic temperature (T_{iso}) and the intercept $a = \ln k_{iso}$ is related to the isokinetic rate constant (k_{iso}).

The appearance of the IKR shows that only one mechanism is present, whereas the existence of parameters that do not agree with the IKR implies that there are multiple reaction mechanisms [37]. In accordance with certain authors [36], we selected the reaction model whose IKR in relation to the conversion had the best linear correlation coefficient and in which the associated T_{iso} value was near the experimental temperature range.

Vyazovkin and Linert [36] claims that the real pre-exponential factor can be predicted by using the isoconversional apparent activation energy and the compensation effect in relation to the reaction model, at an average heating rate, without needing to know the analytical form of reaction model. The most suitable reaction model is that, which presents the lowest error or deviation in equation of the following form:

$$\Delta(\%) = 100 \frac{1}{N} \sum_{\alpha} \frac{|\ln A_{\alpha,pred} - \ln A_{\alpha,isocon}|}{\ln A_{\alpha,pred}} \quad (10)$$

where N represents the number of elements for which the deviation is calculated, $\ln A_{\alpha,pred}$ is the predicted pre-exponential factor based on the IKR in relation to the reaction model and $\ln A_{\alpha,isocon}$ is the pre-exponential factor calculated by applying the reaction model to the isoconversional data.

3.5. Invariant kinetic parameters method (IKP method)

In this article, the method proposed by Budrugeac et al. [38] was used for the purpose of determining the invariant kinetic parameters (IKP). The method is based on the experimental observation that the same thermoanalytical curve can be described relatively fair by the several different conversion functions.

Using an integral (Coats–Redfern (CR)) method (Eq. (6)), for each heating rate and for each conversion function, a pair of kinetic parameters (A , E_a) is established. Using the artificial compensation effect that always exists when the reaction model changes, for each heating rate, the compensation parameters, a_v and b_v , are determined in accordance with Eq. (9) (often used for parameters and designations as α_v^* and β_v^* [38]). The point of intersection of the straight lines of compensations for several heating rates corresponds to the real values of E_a and A , called the invariant kinetic parameters ($E_{a,inv}$ and A_{inv}), as they are independent of the conversion, the model and the heating rate [38]. Since determining the point of intersection by the graphical method means is uncertain, the invariant kinetic parameters can be defined by the corresponding supercorrelation relation:

$$a_v = \ln A_{inv} - b_v E_{a,inv} \quad (11)$$

The straight line a_v versus b_v allows us to determine the invariant kinetic parameters ($E_{a,inv}$ and A_{inv}) from the slope and the intercept.

Although, the IKP method aims to determine the invariant kinetic parameters independently of the reaction model, comparing them to those obtained using the other methods (such as CR method, isoconversional methods, etc.), also allows us to decide which reaction model best describes the investigated degradation process.

3.6. Integral master plot method

Using the reference point at $\alpha = 0.50$, the following integral master equation can be derived from Eq. (3):

$$\frac{g(\alpha)}{g(0.50)} = \frac{p(x)}{p(x_{0.50})} \quad (12)$$

where $p(x_{0.50})$ is the temperature integral at the value of $\alpha = 0.50$. In this article, the fourth rational approximation of Senum and Yang [28] is used for $p(x)$. Recently, some authors [39,40] have given universal expression to the master plot using the concept of generalized time introduced by Ozawa [23]. The particularization of the generalized kinetic equation for the non-isothermal experiments leads to Eq. (12).

In order to determine the reaction model, it is necessary that the conversion function $f(\alpha)$, which is characteristic for the investigated process, should be included in the analyzed set of analytical functions. Different reaction models were studied for the purpose of determining the most suitable $f(\alpha)$ (or $g(\alpha)$) function, which best describes the non-isothermal degradation process of the cured Primaset® PT-30 resin. These models are the follows: power law (P1, P2, P3 and P4), phase-boundary-controlled reactions (R1, R2 and R3), reaction order (n) models ($n = 1, 3/2, 2$ and 3 with labels F1, F3/2, F2 and F3), Avrami–Erofeev reaction models (A3/2, A2, A3 and A4) and diffusion models (D1, D2, D3 and D4) [41].

4. Results and discussion

Fig. 1 shows the experimentally obtained non-isothermal thermogravimetric (TG) (a) and differential thermogravimetric (DTG) (b) curves at the different heating rates ($\beta = 0.01, 0.10, 1, 10$ and

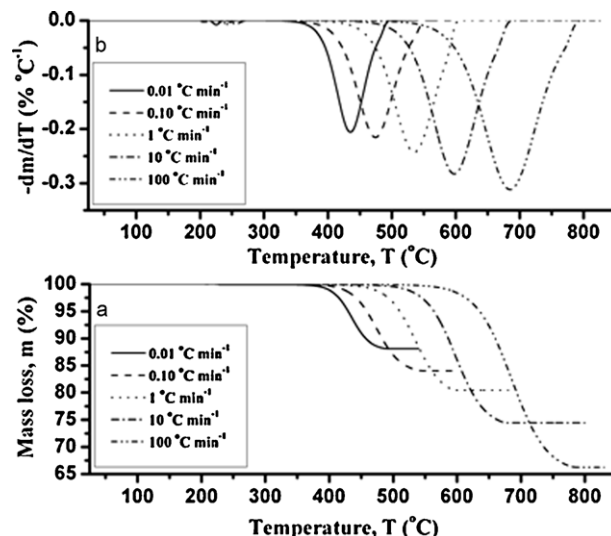


Fig. 1. The experimentally obtained thermogravimetric (TG) (a) and differential thermogravimetric (DTG) (b) curves at the different heating rates ($\beta = 0.01, 0.10, 1, 10$ and $100^\circ\text{C min}^{-1}$), for the degradation process of the cured Primaset® PT-30 resin.

$100^\circ\text{C min}^{-1}$), for the degradation process of the cured Primaset® PT-30 resin.

It can be seen from Fig. 1 that with increasing heating rate, TG and DTG curves are shifted to higher experimental temperatures, which is a typical case of thermally activated heterogeneous process. On the other hand, we can see that the total mass loss of the sample strongly depends on the heating rate, where this loss is very small at the lowest heating rate ($0.01^\circ\text{C min}^{-1}$), while the biggest loss may be seen at the highest heating rate of the system ($100^\circ\text{C min}^{-1}$). As can be seen, that the total mass loss rises with increasing heating rate, then this effect may be an indication of the complex process that contains at least two steps, whereas the last step consists of two concurrent processes with different apparent activation energies. The total mass loss may depend on the heating rate, because of the different apparent activation energies of the two processes. However, the above hypothesis about the reaction mechanism can not be seen from the corresponding DTG curves, bearing in mind that these curves are characterized by one main peak, whose width and asymmetry gradually increases with the increase in the heating rate (β).

Table 1 shows the values of characteristic degradation temperatures (the onset (initial) degradation temperature (T_i), the maximum (peak) degradation temperature (T_p) and the final degradation temperature (T_f)), the total mass loss values (Δm) and the values of degradation rates ($d\alpha/dt$), at the different β s. T_i is taken as the point where the thermogram starts to show an inflex. T_p is taken from the differential thermogravimetric (DTG) curves (Fig. 1(b)) and T_f , the temperature at which TG curve tends to attain a plateau region for considered process.

Table 1 shows that with increase in heating rates (β), the values of characteristic degradation temperatures (T_i , T_p and T_f) also

Table 1

The values of characteristic temperatures (T_i , T_p and T_f), the total mass losses (Δm) and the rates ($d\alpha/dt$) of the degradation process of the cured Primaset® PT-30 resin in nitrogen atmosphere, at different heating rates ($\beta = 0.01, 0.10, 1, 10$ and $100^\circ\text{C min}^{-1}$).

β ($^\circ\text{C min}^{-1}$)	T_i ($^\circ\text{C}$)	T_p ($^\circ\text{C}$)	T_f ($^\circ\text{C}$)	Mass loss, Δm (%)	$d\alpha/dt$ (min^{-1})
0.01	325.00	435.96	485.61	12.00	1.654×10^{-4}
0.10	350.00	474.09	534.80	16.00	0.00130
1	400.00	534.44	589.24	20.00	0.01114
10	450.00	596.46	673.38	26.00	0.10380
100	525.00	683.64	784.34	34.00	0.90600

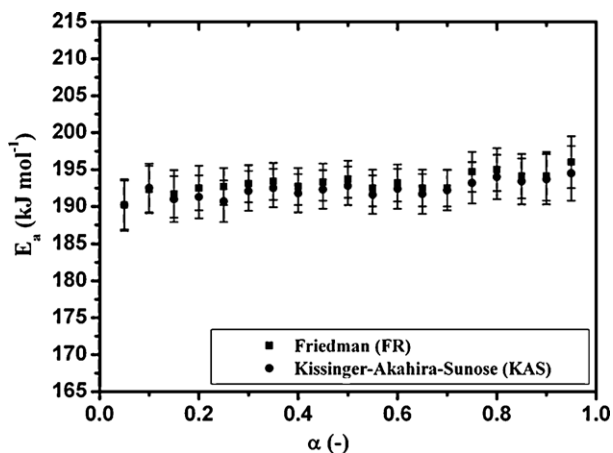


Fig. 2. The dependence of the apparent activation energy (E_a) on the degree of conversion (α), for the non-isothermal degradation of the cured Primaset[®] PT-30 resin, calculated by the FR and KAS isoconversional methods (Eqs. (4) and (5)).

increase. Furthermore, the values of the total mass loss and degradation rate, also increases with increasing heating rate of the system. The total mass loss of the sample at $\beta = 100^\circ\text{C min}^{-1}$ is almost three times greater than the mass loss at $\beta = 0.01^\circ\text{C min}^{-1}$ (Table 1), which confirms its strong dependence on the heating rate (β).

It can be observed from Table 1, that the onset degradation temperatures at all heating rates are high, which is a significant indication for the proposition that the cyanurates are the thermally stable cross-links that are responsible for the high mass loss temperature ($>350^\circ\text{C}$) of this thermoset. These results (Table 1) confirm a proven fact that the cyanate ester resins can be used for the high temperature applications [42]. The char residues were present at the end of each thermoanalytical experiment. It can be pointed out, that the char yield is sensitive to the chemical structure of the monomer and increases with glass transition temperature and in rough proportion to the mole fraction of unsaturated carbon-carbon bonds [43]. It was shown that the nitrogen and oxygen in the cyanurate ring are incorporated into the char, but at an efficiency that is 2–3 times higher than fused-aromatic heterocycles such as the benzimidazoles and phenylquinioxalines [43]. Alternatively, the cyanurate could be interacting with other structural groups to increase their char-forming tendency during the process of thermal degradation.

At higher heating rates (at 10 and $100^\circ\text{C min}^{-1}$) degradation processes are running faster and more vigorously (Table 1, Column 6).

In order to determine realistic and accurate kinetic triplet for non-isothermal degradation of the cured Primaset[®] PT-30 resin, the first step in the kinetic analysis is the use of isoconversional methods. These methods allow verification of the presence or absence of the complexity of investigated process, tested from the mechanistic point of view. In this case, we can check whether the apparent activation energy shows the dependence on the degree of conversion (α) in the whole range of α values, or only a part of it.

Fig. 2 shows the dependence of the apparent activation energy (E_a) on the degree of conversion (α), which was obtained by FR and KAS isoconversional methods (Eqs. (4) and (5)). It can be seen from Fig. 2 that the apparent activation energy values vary very slightly around a mean value. These mean values of E_a in the range $0.10 \leq \alpha \leq 0.90$, calculated by the FR and KAS methods are equal $E_{aFR} = 193.2 \text{ kJ mol}^{-1}$ and $E_{aKAS} = 192.3 \text{ kJ mol}^{-1}$, respectively. It may be noted that there is good agreement between the values of the apparent activation energy obtained by the FR and KAS methods.

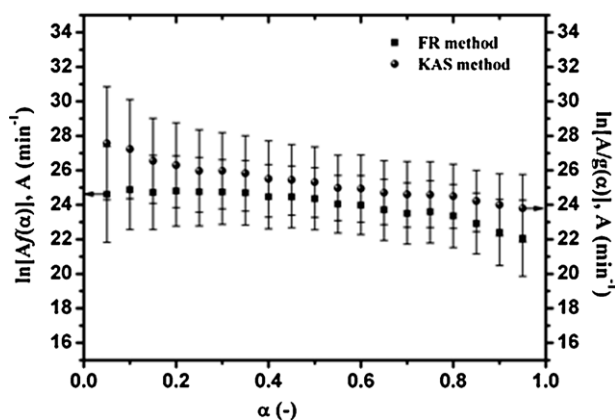


Fig. 3. The dependence of the isoconversional intercepts ($\ln[A/f(\alpha)]$ and $\ln[A/g(\alpha)]$) on the degree of conversion (α), for the non-isothermal degradation of the cured Primaset[®] PT-30 resin, evaluated from FR and KAS isoconversional methods.

From the results presented in Fig. 2, we can conclude that the degradation process of the cured Primaset[®] PT-30 proceeds through a single reaction step, which allows us to determine the function of the kinetic model. Namely, if E_a is independent of α , then the FR and KAS methods give practically the same values of the apparent activation energy [44]. It can be said that the above condition is fulfilled in the case of our investigated degradation process. In the case of the cured Primaset[®] PT-30 resin, based on the obtained values of E_a , we can say preliminarily that the degradation process most likely involves thermolytic cleavage of the resin backbone (usually occurred in the temperature range of $325\text{--}450^\circ\text{C}$), which is probably accompanied by the decyclization of the triazine rings (occurred in the temperature range of $450\text{--}500^\circ\text{C}$) with liberation of low molecular mass volatile compounds (for this type of reaction, the apparent activation energy values are typically ranging from $E_a = 120 \text{ kJ mol}^{-1}$ to $E_a = 220 \text{ kJ mol}^{-1}$) [2,45–48]. Such an assumption is made, since the high value of E_a ($E_a = 192.3 \text{ kJ mol}^{-1}$) can not be obtained from the reaction of aliphatic components, but from the reactions involving bridges connecting the aromatic rings, or the aromatic rings, independently. This discussion should be accepted as a hypothesis, because the precise mechanism of degradation can be assessed only after determining the exact form of the $f(\alpha)$ (or $g(\alpha)$) function.

It should be noted that the isoconversional intercepts show a similar dependence on α (Fig. 3 (for the FR and KAS methods)) as well as the apparent activation energy values. Also, it should be noted that the values of the pre-exponential factors (A) can be obtained, only if we know the exact analytical form of the $f(\alpha)$ (or $g(\alpha)$) function.

By introducing the various analytical forms of $g(\alpha)$ and $f(\alpha)$ functions for analyzed kinetic models [41] in Eqs. (7) and (8) at all heating rates (β), the following best models were selected: the first order (F1) and one and a half-order (F3/2) kinetic models. Fig. 4 shows the results for F1 and F3/2 kinetic models, obtained from the composite integral and differential method I.

Table 2 shows the values of the kinetic parameters (A and E_a) together with results evaluated from the regression analysis (corresponding R^2 values), using the composite integral and differential method I (Eqs. (7) and (8)), for the non-isothermal degradation of the cured Primaset[®] PT-30 resin in nitrogen atmosphere.

It can be seen from Table 2, that the values of E_a for the F3/2 model calculated by the composite integral and differential method I ($E_a^{int} = 193.8 \text{ kJ mol}^{-1}$ and $E_a^{diff} = 196.8 \text{ kJ mol}^{-1}$, respectively) are closest to the value of E_a , obtained from the isoconversional analysis ($E_{aFR} = 193.2 \text{ kJ mol}^{-1}$). On the other hand, the composite differential method I give, for the F3/2 model, the value of A which is for

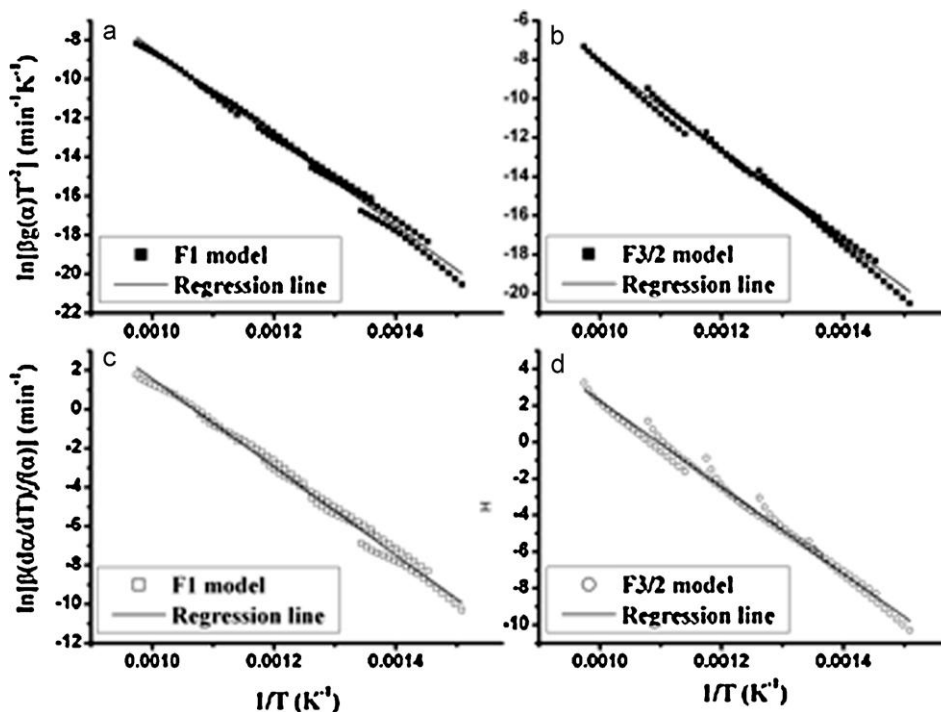


Fig. 4. Composite integral ((a) and (b)) and differential ((c) and (d)) method I analysis of the non-isothermal thermoanalytical data ($\beta = 0.01, 0.10, 1, 10$ and $100^\circ\text{C min}^{-1}$) for F1 and F3/2 models.

Table 2

Kinetic parameters (E_a, A) determined using the composite integral and differential method I (Eqs. (7) and (8)) for the degradation process of the cured Primaset® PT-30 resin in nitrogen atmosphere ($R^2 = \text{Adj. } R\text{-square}$).

Kinetic parameters	Composite integral method I		Composite differential method I	
	F1 model	F3/2 model	F1 model	F3/2 model
E_a (kJ mol $^{-1}$)	188.9	193.8	187.9	196.8
$\ln A$	24.32	25.31	24.16	25.94
A (min $^{-1}$)	3.65×10^{10}	9.82×10^{10}	3.11×10^{10}	1.84×10^{11}
R^2	0.99349	0.99403	0.99298	0.99275

one order of magnitude greater than the value of A calculated by the composite integral method I (Table 2).

It should be noted, that the data does not totally overlap (Fig. 4), which suggests that the methods that mix integral and differential data will lead to the results that are not very precise. Using integral and differential data separately, however, allows us to establish the kinetic model reasonably well, and for the investigated degradation process, the best results are obtained from the integral data. In accordance with these facts, Criado et al. [35] demonstrated that for the thermal degradation of a solid sample, composite methods allow us to differentiate between kinetic models, which can correctly, reproduces the thermally activated process despite having the different kinetic parameters. In accordance with these authors, the kinetic model in which the data are grouped together in just one straight line (Eq. (7)) is the correct one and the kinetic parameters obtained from this straight line are the real ones. Accepting this hypothesis as the correct, we take a kinetic model F3/2 with E_a and A values presented in Table 2 ($E_a^{\text{int}} = 193.8 \text{ kJ mol}^{-1}$; $A = 9.82 \times 10^{10} \text{ min}^{-1}$), which were obtained from overlapping data to the one single master integral curve (Fig. 4).

As a criterion to perform the reliable kinetic model, the existence of IKR can be used when the conversion changes, together with the fact that the T_{iso} is within the experimental range of temperatures.

Table 3 shows the results obtained using the IKR and Eq. (10) from the integral data, for the non-isothermal degradation of the cured Primaset® PT-30 resin in nitrogen atmosphere.

We can see from Table 3 that the many kinetic models have T_{iso} in the experimental range of temperatures. However, on the other hand, the error Δ (%) (that occurs when comparing the pre-exponential factors estimated from the IKRs when the conversion

Table 3

Compensation effect in relation to conversion (Eq. (9)) with corresponding values of Δ (in %) (Eq. (10)), for non-isothermal degradation process of the cured Primaset® PT-30 resin in nitrogen atmosphere.

Model	a (min $^{-1}$)	b (mol kJ $^{-1}$)	T_{iso} ($^\circ\text{C}$)	Δ (%)
P1	9.65988	-0.61501	-468.73	16.7
P2	9.07825	-0.31189	-658.81	15.2
P3	4.67219	-0.0308	-4178.32	15.7
P4	-4.30763	0.14724	543.73	16.9
R1	-2.27151	0.1294	656.35	13.6
R2	-4.28732	0.14419	561.01	9.3
R3	-4.88085	0.1465	547.86	7.7
F1	-3.65524	0.14752	542.18	0.8
F3/2	-2.71279	0.14514	555.55	0.2
F2	-0.61405	0.13895	592.47	5.6
F3	5.27382	0.12676	675.71	6.1
A3/2	-3.32162	0.14122	578.55	1.8
A2	-1.85882	0.11698	755.04	1.4
A3	1.91884	0.01159	10104.67	2.1
A4	4.88376	-0.15097	-1069.87	2.8
D1	-4.62799	0.14847	536.96	4.5
D2	-4.09453	0.14539	554.13	3.3
D3	-3.47998	0.14041	583.47	8.0
D4	-4.99128	0.14393	562.52	7.9

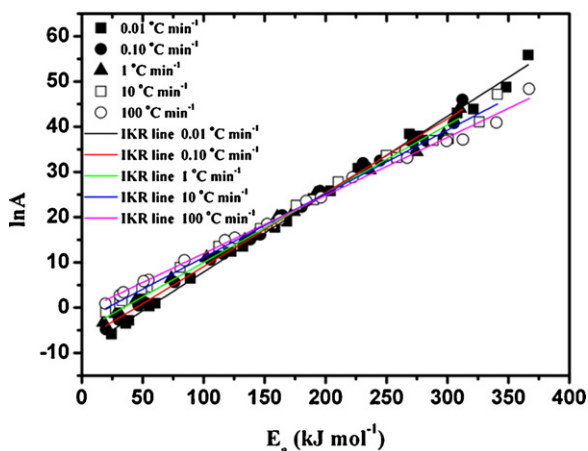


Fig. 5. The artificial IKR plots obtained from the Coats–Redfern method at the different heating rates ($\beta = 0.01, 0.10, 1, 10$ and $100^\circ\text{C min}^{-1}$), for the non-isothermal degradation of the cured Primaset[®] PT-30 resin (the corresponding IKR lines at a given heating rates are designated with color lines).

changes to the factors predicted from the IKRs when the model changes) is lowest for models F3/2 and F1, which are suitable for further computational procedure (Table 3). This approach does not allow us to establish the kinetic model unambiguously, but provides the information which family of the analytical functions of kinetic models best describes the investigated degradation process.

In order to establish the invariant kinetic parameters and decide which kinetic model best describes the degradation process of the cured Primaset[®] PT-30 resin, we can also take advantage of the IKR method. The artificial IKR [36] plots obtained from the Coats–Redfern method (Eq. (6)) at the different heating rates ($\beta = 0.01, 0.10, 1, 10$ and $100^\circ\text{C min}^{-1}$), for the non-isothermal degradation of the cured Primaset[®] PT-30 resin are presented in Fig. 5.

It can be seen from Fig. 5 that the IKR lines at all considered heating rates are intersect at one point, or in other words the linear relationships (colored lines in Fig. 5) tend to converge to one point called IKR point either NP as the narrowest point [36,49]. This point is taken as the characteristic point for all non-isothermal experiments. In addition, the mentioned point (with the pairs of $\ln A$ and E_a values) (Fig. 5) can be accurately determined by applying the invariant kinetic parameters method (IKP method).

Table 4 shows the values of the invariant compensation parameters, a_v and b_v , with the corresponding values of T_{iso} ($b_v = 1/RT_{iso}$) calculated from the linear plots in Fig. 5.

It can be observed from Table 4 that the calculated values of T_{iso} at different heating rates are similar to those obtained in the IKRs established when changing the conversions for the models F3/2 and F1 (just look at these models because they give the smallest error values, Δ (%)).

The invariant kinetic parameters established from the data in Table 4 using the supercorrelation of Eq. (11) are $E_{a,inv} = 192.1 \text{ kJ mol}^{-1}$, $\ln A_{inv} = 23.95$ ($A_{inv} = 2.52 \times 10^{10} \text{ min}^{-1}$), $R^2 = 0.99638$. These parameters are very close to the values of

Table 4

The values of the integral compensation parameters (a_v and b_v), obtained from the Coats and Redfern method (Fig. 5), at the different values of heating rates (0.01, 0.10, 1, 10 and $100^\circ\text{C min}^{-1}$).

β ($^\circ\text{C min}^{-1}$)	a_v (min^{-1})	b_v (mol kJ^{-1})	T_{iso} ($^\circ\text{C}$)	R^2
0.01	-9.30166	0.17202	426.05	0.99711
0.10	-7.24976	0.16340	462.94	0.99578
1	-5.17748	0.15192	518.57	0.99498
10	-2.93337	0.14066	581.95	0.99510
100	-0.83719	0.12826	664.61	0.99462

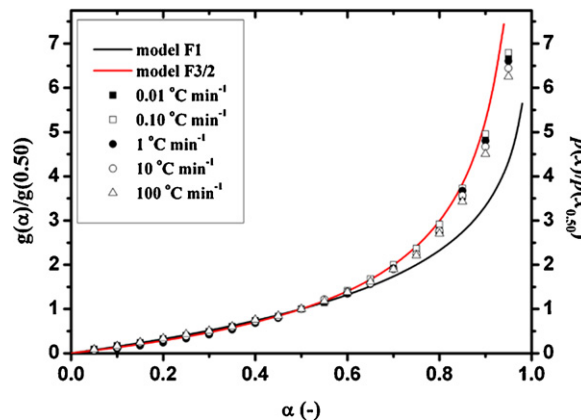


Fig. 6. The comparison between the theoretical integral master curves for F1 (full black line) and F3/2 (full red line) kinetic models and the experimental master curves (symbols) that are derived using the constant value of E_a , calculated from the IKP method ($E_a = 192.1 \text{ kJ mol}^{-1}$), in the conversion range of $0.05 \leq \alpha \leq 0.95$.

kinetic parameters obtained by the integral (KAS) isoconversional method as well as the composite integral method I (Table 2), for the clearly separated F3/2 kinetic model.

This analysis allows us to establish unique 'kinetic triplet' for the range of conversions where E_a does not shows any significant variation, and therefore we can choose the F3/2 model to describe the observed degradation process.

In order to confirm the selected kinetic model, we can apply the integral master plot method, which is defined by the Eq. (12). Fig. 6 shows the theoretical integral master curves for F1 (full black line) and F3/2 (full red line) models, and also the experimental master curves (symbols) that are derived using the constant value of E_a , calculated from the IKP method ($E_{a,inv} = 192.1 \text{ kJ mol}^{-1}$), in the range of $0.05 \leq \alpha \leq 0.95$.

It can be seen from Fig. 6 that the experimental master curves (at all heating rates) are in good agreement with theoretical master curve for F3/2 model. However, we note that there is a small deviation at the higher values of α (for $\alpha \geq 0.80$), at all considered heating rates. The observed deviations at higher values of conversion can originated from the sentient impact of the heating rate (β).

In addition, Fig. 7 shows the comparison between the experimentally obtained differential ($d\alpha/dT - T$) degradation curves and the calculated $d\alpha/dT - T$ curves, using the Eq. (1) with the following values of the kinetic triplet: $E_a = 193.8 \text{ kJ mol}^{-1}$, $A = 9.82 \times 10^{10} \text{ min}^{-1}$ and $f(\alpha) = (1 - \alpha)^{3/2}$.

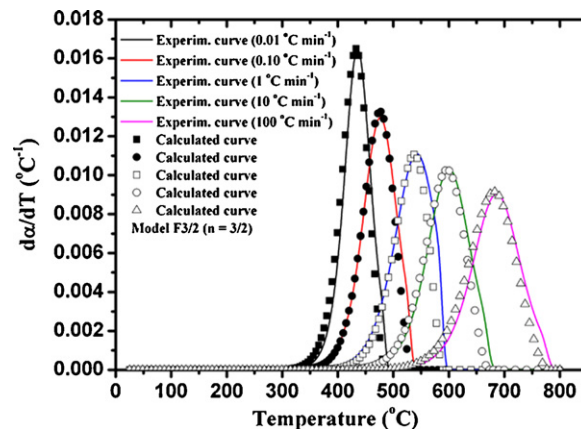


Fig. 7. The comparison between the experimentally obtained differential ($d\alpha/dT - T$) degradation curves (color curves) and the calculated $d\alpha/dT - T$ degradation curves (symbol curves), using the Eq. (1) with the following 'kinetic triplet' as: $E_a = 193.8 \text{ kJ mol}^{-1}$, $A = 9.82 \times 10^{10} \text{ min}^{-1}$ and $f(\alpha) = (1 - \alpha)^{3/2}$.

It can be clearly seen from Fig. 7 that for the values of the above-derived kinetic parameters and for one and a half order mechanism (F_n , $n = 3/2$), the experimental differential ($d\alpha/dT - T$) degradation curves may be successfully simulated, so that the investigated degradation process could be unambiguously described from a mechanistic point of view.

We should mention that when we have the presence of the degradation process that involves the random scission, the kinetics will probably deviate from a first-order ($n = 1$) model [50,51]. Taking into account our tested system, the random scission mechanism was probably included in the process of degradation of the cured Primaset® PT-30 resin (F_n kinetic model with $n = 3/2$). On the other hand, the higher apparent activation energy (193.8 kJ mol⁻¹) of the non-isothermal degradation of the cured Primaset® PT-30 resin, when the order of reaction is fractional, also may indicate a stabilization of the cured PT-30 resin during the considered process, through the cross-linking of the hydrocarbon backbone. Since, that the cleavage of the first bonds will not immediately result in evaporation of the degraded chains, so that the process can be considered in the presence of some initiation period with a comparatively low conversion rate. Following this initiation period, the conversion rate first increases until it reaches a maximum and then decreases due to a decrease of the available number of bonds. Bearing in mind that the kinetics of the cured Primaset® PT-30 resin degradation deviates from the simple first-order reaction mechanism, we can conclude that the investigated process according to its kinetic nature, is actually complex. Considering that at the end of the non-isothermal experiments (which were carried out at higher temperature regimes) was observed higher amounts of char residues (with lower loss in mass of the sample in general, but which nevertheless progressive increases with increasing in heating rate (Table 1)), the fractional n th order kinetic model ($n = 3/2$) probably includes random scission reaction followed with decyclization of the cyanurate rings producing volatile compounds and corresponding char residue whose amounts depends on the aromatic content of the polycyanurate backbone. This is confirmed by the fact that the reaction order n obtained from the detailed kinetic analysis is not equal to unity, which illustrates that the reaction mechanism is complicated.

Due to the complex nature of this degradation mechanism of the cured Primaset® PT-30 resin, its kinetics is not possible to be described with zero, first or second order kinetics equations. Since, that not every broken bond in the chain leads to the volatilization of the products, only product fragments which are small enough to volatile will actually volatile at the given reaction temperature and thus lead to a decrease of the resin mass. This implies that both physical and chemical processes influence the measured rate of change of the resin sample mass and hence the observed degradation kinetics.

It can be pointed out that the degradation of polycyanurates in inert (N₂) atmosphere between 300 °C and 600 °C may cause the porous material [2]. Little shrinkage can be observed in this temperature range. Thermal degradation slightly below 300 °C in inert atmosphere produces small amounts of gaseous products [6]. These are mostly unreacted monomers, which are by-products eliminated from the condensation reactions between hydroxymethyl groups and reactive ortho or para positions on phenolic rings.

Based on the presented results, with the “quasi” single step reaction model (F_n -type), a complex and multi-step non-isothermal degradation process of the cured Primaset® PT-30 resin in nitrogen atmosphere can be successfully approximated. Kinetic triplet from the NP point (IKP method) or from the composite integral method I can be successfully used for the non-isothermal simulations of the investigated degradation process as a “quasi” single step reaction model.

Isoconversional methods can be used to predict the isothermal kinetics. Vyazovkin [20] proposed a “model-free” method that allows us to use non-isothermal data for predicting isothermal kinetics. This method is based on the following equation [20]:

$$t_\alpha = \left[\beta \exp\left(-\frac{E_{a,\alpha}}{RT_0}\right) \right]^{-1} \sum_0^\alpha \int_{T_{\alpha-\Delta\alpha}}^{T_\alpha} \exp\left(-\frac{E_{a,\alpha}}{RT}\right) dT \quad (13)$$

where t_α represents the time, at which a given conversion will be reached at an arbitrary isothermal temperature, T_0 . β is the heating rate of the non-isothermal experiment used in calculation procedure, $E_{a,\alpha}$ represents the apparent activation energy values calculated for a given value of α ($E_{a,\alpha}$ is usually taken from the FR method [52]), T_α represents the temperature value for a given degree of conversion (α), $\Delta\alpha$ represents the small conversion interval and R is the gas constant. In Eq. (13), α is varied from $\Delta\alpha$ to $1 - \Delta\alpha$ with a step $\Delta\alpha = s^{-1}$, where s is the number of intervals chosen for analysis. Note that according to Eq. (13), each value of t_α is predicted by using the respective value of $E_{a,\alpha}$.

The integral (KAS) isoconversional method (Eq. (5)) assumes that the value of $E_{a,\alpha}$ is constant in the temperature integral throughout the whole interval of integration, from 0 to α . This assumption causes a systematic error in the value of $E_{a,\alpha}$, when $E_{a,\alpha}$ varies with α . However, this error does not appear in the differential Friedman's isoconversional method. Furthermore, the mentioned error can be easily eliminated using the advanced integral method of Vyazovkin [53–55], because it uses the numerical integration as a part of $E_{a,\alpha}$ evaluation. Eliminating errors in Vyazovkin method was achieved by the integration over small temperature segments as follows:

$$I(E_{a,\alpha}, T) = \int_{T_{\alpha-\Delta\alpha}}^{T_\alpha} \exp\left(-\frac{E_{a,\alpha}}{RT}\right) dT \quad (14)$$

where $I(E_{a,\alpha}, T)$ represents the temperature integral on the right-hand side of Eq. (13). In this case, $E_{a,\alpha}$ is assumed constant for only a small interval of conversions, $\Delta\alpha$. Integration by segments yields $E_{a,\alpha}$ values that are similar to those obtained by the Friedman method [54].

To solve the integral in Eq. (13), we used the numerical integration by the trapezoidal rule [56], for a set of the experimental heating programs. Predictions made by the Eq. (13) can be called “model-free predictions” because it does not require knowledge of the reaction model (or the pre-exponential factor). Eq. (13) can be applied for determination of lifetime (t_f) of a resin to failure. Lifetime estimations using TG technique are useful in the processing and in the development or selection of resins for different applications where long-term usage is essential.

Fig. 8 shows the comparison between the “model-free” predicted conversion curves (using the Eq. (13)) and the experimentally obtained conversion curves (that were presented on the logarithmic time scale), at the isothermal temperatures of $T_0 = 400$ °C, 420 °C and 450 °C. The results obtained from the Friedman's isoconversional method are used for the isothermal predictions at all considered temperatures. For the isothermal predictions of the cured Primaset® PT-30 resin degradation process, the heating rate values of $\beta = 0.10$ °C min⁻¹ and $\beta = 10$ °C min⁻¹ were used.

It can be observed that all isothermal predicted curves are similar in the shape with experimental curves, but the predicted curves require a longer times for degradation process (Fig. 8) (shift towards to higher t values on a logarithmic scale). With increase in operating temperature (T_0), time for degradation of the cured Primaset® PT-30 resin decreases, which can be confirmed the high thermal stability of the tested resin imparted by the phenyl rings. The relatively high value of the apparent activation energy that was obtained for the investigated degradation process (results for $E_{a,\alpha}$

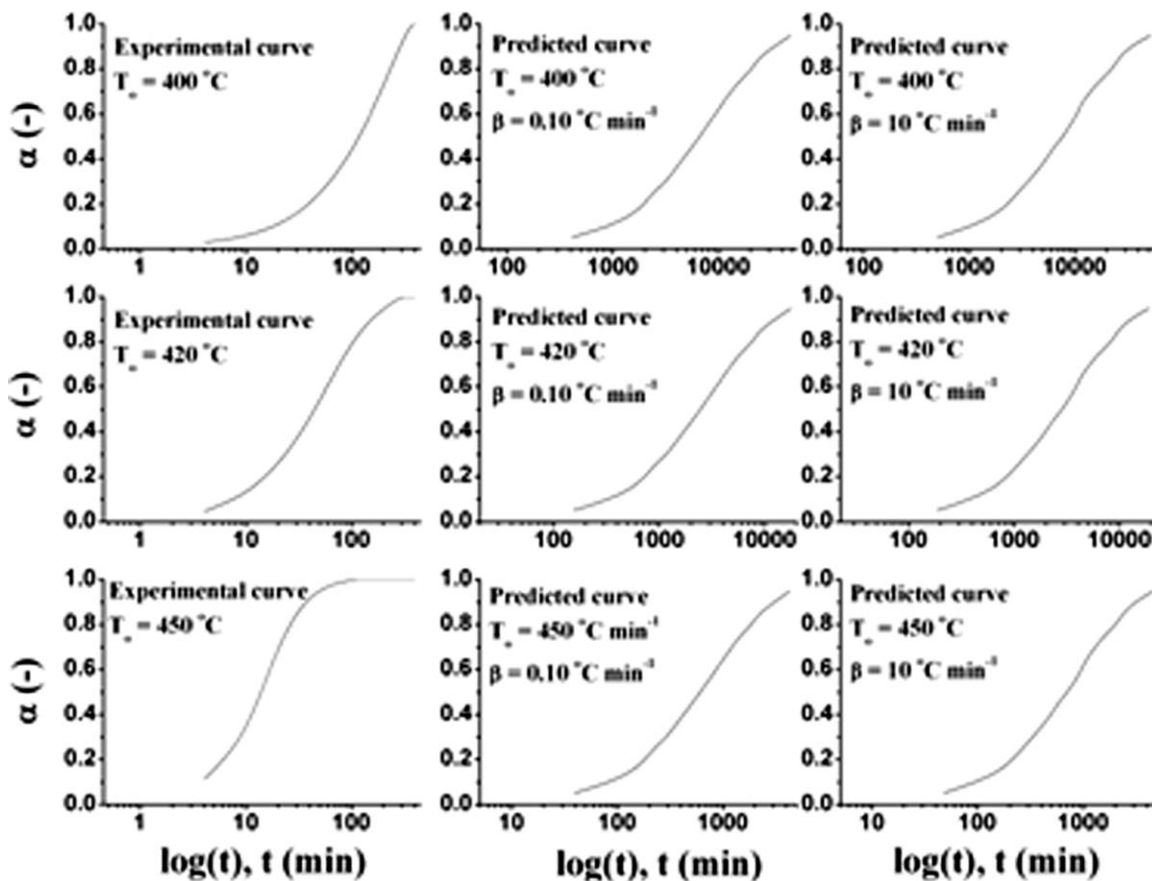


Fig. 8. The comparison between the “model-free” predicted conversion curves (using the Eq. (13)) and the experimentally obtained isothermal conversion curves with logarithmic time scales ($\log(t)$), at the operating temperatures of $T_0 = 400, 420$ and 450 °C. For the isothermal prediction analysis, the heating rate values of $\beta = 0.10$ °C min^{-1} and $\beta = 10$ °C min^{-1} were used.

from the KAS and FR methods) and predicted times of degradation at the considered isothermal temperatures, leads us to conclude that the cured Primaset® PT-30 resin has high thermal resistance, which means, that the Primaset® PT-30 needs more temperature to process it to produce parts for usage.

Disagreement between the prediction curves and experimental curves in terms of degradation lifetime at the observed temperatures could lay in a very strong dependence of the observed reaction system on the heating rate, which means on the temperature of degradation. The deviation at intermediate and higher conversions may arise from the use of very high value of heating rate (e.g. $\beta = 100$ °C min^{-1}), so the results may be subject to the influence of mass and heat transfers. However, using the lower values of heating rates lead to more adjusted $\alpha(t)$ curves.

In addition, all the kinetic calculations are based on the relative degree of conversion that always varies within the range of $0 \leq \alpha \leq 1$, despite the fact that the absolute degree of conversion decreases with the temperature [57]. For incomplete cures, the isoconversional methods yield the correct values of the apparent activation energy provided the relative degrees of conversion of the cure are used instead of the absolute values [57]. In this case, it is likely that the actual measurements appear much faster than the predictions, because the same conversion, corresponds to perhaps twice smaller actual mass loss at the temperature of prediction (i.e. 400, 420 and 450 °C) than at the heating rates that were used for prediction (Fig. 8). Nevertheless, it is noticeable that the mass loss in the thermogravimetric measurements depends strongly on the heating rate. By the transformation $\alpha = (m_0 - m)/(m_0 - m_f)$ to the range of values $0 \leq \alpha \leq 1$, this specific behavior of the measurements is lost, i.e. one loses the dependence of the total mass loss on

the heating rate. Therefore, the “model-free” analysis cannot provide a prediction [57] that also calculates different mass losses at the different heating rates. Consequently, the “quasi” single step reaction model (Fn-type) looks like a reasonable approximation to describe the kinetics of the complex degradation process of the cured Primaset® PT-30 resin.

The estimated lifetime (t_f) of a cured resin can be defined as the time when the mass loss reaches 5 wt%, i.e. $\alpha = 0.05$ [58]. From the integration of Eq. (15):

$$\frac{d\alpha}{dt} = A \exp\left(\frac{-E_a}{RT}\right) (1 - \alpha)^n \quad (15)$$

(n is the reaction order), the lifetime can be estimated for $n \neq 1$ in the form:

$$t_f = \frac{1 - 0.95^{1-n}}{A(1-n)} \exp\left(\frac{E_a}{RT}\right) \quad (16)$$

The reaction order value n , can be obtained directly from the symmetrical index of a derivative thermogravimetry (DTG) peak based on the second Kissinger technique [59]:

$$n = 1.88 \cdot \frac{|(d^2\alpha/dt^2)_L|}{|(d^2\alpha/dt^2)_R|} \quad (17)$$

where indices L and R correspond to the left and right peak ($d^2\alpha/dt^2$) values (extrema) on the second derivative thermogravimetry (DDTG) curves.

Table 5 shows the reaction order (n) values at various heating rates for degradation process of the cured Primaset® PT-30 resin in nitrogen atmosphere, which were obtained from DDTG curves using Eq. (17). In the same table (Table 5), $\ln A$ values calculated

Table 5

Non-isothermal degradation kinetic parameters of the cured Primaset® PT-30 resin at a mass loss of 5%.

Heating rate, $\beta/^\circ\text{C min}^{-1}$	Atmosphere	Reaction order, n	E_a (kJ mol $^{-1}$)	lnA
0.01	Nitrogen (N $_2$)	1.52	190.2	24.23
0.10		1.56		24.96
1		1.20		23.25
10		1.68		25.63
100		1.48		24.09
Average		1.49		24.43

Table 6

Estimation values of lifetime of the cured Primaset® PT-30 resin degradation, based on the kinetic data from Table 5 and by applying the Eq. (16).

Atmosphere	Lifetime, t_f (min at temperature)								
	25 °C	100 °C	200 °C	300 °C	400 °C	500 °C	600 °C	700 °C	800 °C
Nitrogen	2.2256×10^{21}	4.4681×10^{14}	1.0545×10^9	2.2884×10^5	608.7576	7.5073	0.2534	0.0172	0.0019

from Eq. (15) based on the apparent activation energy (E_a) at a mass loss of 5% ($\alpha = 0.05$) are also presented.

The average n and lnA values are 1.49 and 24.43 in nitrogen atmosphere, respectively. These values are in very good agreement with estimated kinetic model with the fractional reaction order ($n = 1.50$; Fn model) and calculated value of lnA from the invariant kinetic parameters method (IKP method).

Using these kinetic data (Table 5) and Eq. (16), the estimation results of the lifetime values for the degradation process of the cured Primaset® PT-30 resin in nitrogen atmosphere at a mass loss of 5% and various temperatures are listed in Table 6.

It is apparent that the lifetime of the cured Primaset® PT-30 resin degradation decreases dramatically from 2.2256×10^{21} min to 0.0019 min as the temperature increases from 25 °C to 800 °C in nitrogen atmosphere.

These lifetime parameters clearly suggest that the service temperature has a strong influence on the degradation process of the cured Primaset® PT-30 resin samples, in a nitrogen atmosphere.

5. Conclusions

The non-isothermal degradation of the cured Primaset® PT-30 resin in nitrogen atmosphere was examined. Thermogravimetry was used to study the mass loss of the solid samples heated at a constant heating rates from $\beta = 0.01^\circ\text{C min}^{-1}$ to $\beta = 100^\circ\text{C min}^{-1}$. It was found that the total mass loss of the sample strongly depends on the heating rate. By using different kinetic methods, the complete kinetic triplet (E_a , A and $f(\alpha)$) of the investigated non-isothermal degradation process was performed. It was found that the degradation process can be successfully described by the following kinetic triplet as: $E_a = 193.8$ kJ mol $^{-1}$, $A = 9.82 \times 10^{10}$ min $^{-1}$ and $f(\alpha) = (1 - \alpha)^{3/2}$. It was concluded that with the single step reaction model (Fn-type) with $n = 3/2$, a complex and multi-step degradation process can be successfully approximated.

The isothermal predictions of the investigated degradation process of the cured Primaset® PT-30 resin were carried out at the temperatures of $T_0 = 400^\circ\text{C}$, 420°C and 450°C . It was established that with increase in operating temperature (T_0), time for degradation of the cured Primaset® PT-30 resin decreases, where it has been concluded that the cured Primaset® PT-30 resin exhibits high thermal stability. It was concluded that due to the high thermal resistance, the Primaset® PT-30 resin needs more temperature to process it to produce parts for usage.

It is proposed that the disagreement between the prediction curves and experimental curves in terms of degradation lifetime at the observed operating temperatures may lie, in a very strong dependence of the observed reaction system on the heating rate. Also, it was assumed that the actual measurements appear

much faster than the predictions, because the same conversion, corresponds to perhaps twice smaller actual mass loss at the temperature of prediction (400, 420 and 450 °C) than at the heating rates that were used for prediction.

The lifetime of the cured Primaset® PT-30 resin degradation decreases dramatically with increase in temperature values. The lifetime parameters indicate that the service/process temperature has a strong influence on the degradation process of the cured Primaset® PT-30 resin under nitrogen atmosphere.

Acknowledgements

The investigation was partially supported by the Ministry of Science and Environmental Protection of Serbia, under the Project 172015. The author wishes to thank MSc Marija Janković for supplying the experimental samples and for performing the thermoanalytical measurements.

References

- [1] S. Das, D.C. Prevorsek, B.T. De Bona, Phenolic-triazine, a versatile high performance thermoset for composite applications, in: 21st Int. SAMPE Tech. Conf., vol. 21, 1989, pp. 972–983.
- [2] C.P. Reghunadhan Nair, D. Mathew, K.N. Ninan, Cyanate ester resins, recent developments, Adv. Polym. Sci. 155 (2001) 1–99.
- [3] S. Lin-Gibson, Cresol novolac/epoxy networks: synthesis, properties, and processability, Doctoral Dissertations, Doctor of Philosophy in Chemistry, Faculty of the Virginia Polytechnic Institute and State University, Blacksburg, VA, USA, 2001, pp. 65–74.
- [4] I. Hamerton, Chemistry and technology of cyanate ester resins, in: I. Hamerton (Ed.), Introduction to Cyanate Ester Resins, vol. 1, Blackie, Glasgow, 1994, pp. 2–5.
- [5] R.T. Conley, Thermal Stability of Polymers, first ed., Marcel Dekker, New York, 1970.
- [6] S. Lin-Gibson, J.S. Riffle, Synthetic methods in step-growth polymers, in: M.E. Rogers, T.E. Long (Eds.), Chemistry and Properties of Phenolic Resins and Networks, vol. 1, John Wiley and Sons, Hoboken, 2003, pp. 418–425.
- [7] J. Fan, X. Hu, C.Y. Yue, Thermal degradation study of interpenetrating polymer network based on modified bismaleimide resin and cyanate ester, Polym. Int. 52 (2003) 15–22.
- [8] R.F. Cozzens, P. Walter, A.W. Snow, Laser pyrolysis of characterized cyanurate network polymers, J. Appl. Polym. Sci. 34 (1987) 601–616.
- [9] M.W. Miks, J.K. Shigly, Addition-polymerisation resin system for fibre reinforced nozzle ablative components, US Patent 5,645,219, Thiokol Corporation, 1997.
- [10] S. Das, D.C. Prevorsek, B.T. De Bona, Phenolic-triazine resins yield high performance thermoset composites, Mod. Plast. Int. 6 (1990) 64–67.
- [11] C.P. Reghunadhan Nair, R.L. Bindu, V.C. Joseph, Cyanate esters based on cardanol modified-phenol-formaldehyde resins: syntheses and thermal characteristics, J. Polym. Sci. A: Polym. Chem. 33 (1995) 621–627.
- [12] P.T. Primaset, Technical Product Brochure, Lonza Ltd, Switzerland, 1996.
- [13] T.R. Manley, Characterization of thermosetting resins by thermal analysis, J. Macromol. Sci. A 8 (1974) 53–64.
- [14] C.A. Gracia-Fernández, S. Gómez-Barreiro, S. Ruiz-Salvador, R. Blaine, Study of the degradation of a thermoset system using TGA and modulated TGA, Prog. Org. Coat. 54 (2005) 332–336.

- [15] R.E. Zacharia, S.L. Simon, Dynamic and isothermal thermogravimetric analysis of a polycyanurate thermosetting system, *Polym. Eng. Sci.* 38 (1998) 566–572.
- [16] J.W. Gilman, R. Harris Jr., Cyanate ester clay nanocomposites: synthesis and flammability studies, in: *Evolving and Revolutionary Technologies for the New Millennium*. Int. SAMPE Symposium/Exhibition, 44th Society for the Advancement of Material and Process Engineering (SAMPE), May 23–27, 1999, Long Beach, CA, 1999, pp. 1408–1423.
- [17] M.L. Ramirez, R. Walters, E.P. Savitski, R.E. Lyon, Thermal decomposition of cyanate ester resins, Final Report DOT/FAA/AR-01/32 for the US Department of Transportation, Washington, DC, September 2001, pp. 1–14.
- [18] M.L. Ramirez, R. Walters, R.E. Lyon, E.P. Savitski, Thermal decomposition of cyanate ester resins, *Polym. Degrad. Stabil.* 78 (2002) 73–82.
- [19] R.L. Sadler, B.D. Morgan, V.S. Avva, Resin transfer molding of 3-D braided through the thickness Pan-based carbon fiber preforms with a cyanate ester, in: *JANNAF Rocket Nozzle Technology Subcommittee Meeting*, Chemical Propulsion Information Agency, Tampa, FL, USA, 1995, pp. 93–101.
- [20] S. Vyazovkin, C.A. Wight, Model-free and model-fitting approaches to kinetic analysis of isothermal and nonisothermal data, *Thermochim. Acta* 340–341 (1999) 53–68.
- [21] F. Paulik, *Special Trends in Thermal Analysis*, first ed., John Wiley and Sons, Chichester, 1995.
- [22] J.H. Flynn, The ‘temperature integral’—its use and abuse, *Thermochim. Acta* 300 (1997) 83–92.
- [23] T. Ozawa, A new method of analyzing thermogravimetric data, *Bull. Chem. Soc. Jpn.* 38 (1965) 1881–1886.
- [24] J.H. Flynn, L.A. Wall, A quick, direct method for the determination of activation energy from thermogravimetric data, *J. Polym. Sci. B: Polym. Lett.* 4 (1966) 323–328.
- [25] H.E. Kissinger, Reaction kinetics in differential thermal analysis, *Anal. Chem.* 29 (1957) 1702–1706.
- [26] T. Akahira, T. Sunose, Joint convention of four electrical institutes, *Res. Rep. Chiba Inst. Technol.* 16 (1971) 22–31.
- [27] M.J. Starink, The determination of activation energy from linear heating rate experiments: a comparison of the accuracy of isoconversion methods, *Thermochim. Acta* 404 (2003) 163–176.
- [28] G.I. Senum, R.T. Yang, Rational approximations of the integral of the Arrhenius function, *J. Therm. Anal. Calorim.* 11 (1977) 445–447.
- [29] P.K. Agarwal, M.S. Sivasubramaniam, Integral approximation for non-isothermal kinetics, *AIChE J.* 33 (1987) 1212–1215.
- [30] H.L. Friedman, Kinetics of thermal degradation of char-forming plastics from thermogravimetry—application to a phenolic resin, *J. Polym. Sci. C: Polym. Lett.* 6 (1964) 183–195.
- [31] A.W. Coats, J.P. Redfern, Kinetic parameters from thermogravimetric data, *Nature* 201 (1964) 68–69.
- [32] S. Vyazovkin, N. Sbirrazzuoli, Isoconversional kinetic analysis of thermally stimulated processes in polymers, *Macromol. Rapid Commun.* 27 (2006) 1515–1532.
- [33] El-H.M. Diefallah, M.A. Gabal, A.A. El-Bellihi, N.A. Eissa, Nonisothermal decomposition of CdC_2O_4 – FeC_2O_4 mixtures in air, *Thermochim. Acta* 376 (2001) 43–50.
- [34] M.A. Gabal, Kinetics of the thermal decomposition of Cu_2O_4 – Zn_2O_4 mixture in air, *Thermochim. Acta* 402 (2003) 199–208.
- [35] J.M. Criado, L.A. Pérez-Maqueda, F.J. Gotor, J. Málek, N. Koga, A unified theory for the kinetic analysis of solid state reactions under any thermal pathway, *J. Therm. Anal. Calorim.* 72 (2003) 901–906.
- [36] S. Vyazovkin, W. Linert, False isokinetic relationships found in the nonisothermal decomposition of solids, *Chem. Phys.* 193 (1995) 109–118.
- [37] S. Vyazovkin, W. Linert, The application of isoconversional methods for analyzing isokinetic relationships occurring at thermal decomposition of solids, *J. Solid State Chem.* 114 (1995) 392–398.
- [38] P. Budrugaec, E. Segal, L.A. Pérez-Maqueda, J.M. Criado, The use of the IKP method for evaluating the kinetic parameters and the conversion function of the thermal dehydrochlorination of PVC from non-isothermal data, *Polym. Degrad. Stabil.* 84 (2004) 311–320.
- [39] N. Koga, J. Málek, J. Šesták, H. Tanaka, Data treatment in non-isothermal kinetics and diagnostic limits of phenomenological models, *Netsu Sokutei* 20 (1993) 210–223.
- [40] F.J. Gotor, J.M. Criado, J. Málek, N. Koga, Kinetic analysis of solid-state reactions: the universality of master plots for analyzing isothermal and nonisothermal experiments, *J. Phys. Chem. A* 104 (2000) 10777–10782.
- [41] A. Khawam, D.R. Flanagan, Solid-state kinetic models: basics and mathematical fundamentals, *J. Phys. Chem. B* 110 (2006) 17315–17328.
- [42] I. Hamerton, J.N. Hay, Recent technological developments in cyanate ester resins, *High Perform. Polym.* 10 (1998) 163–174.
- [43] D.W. Van Krevelen, Some basic aspects of flame resistance of polymeric materials, *Polymer* 16 (1975) 615–620.
- [44] P. Budrugaec, A.L. Petre, E. Segal, Some problems concerning the evaluation of non-isothermal kinetic parameters. Solid–gas decompositions from thermogravimetric data, *J. Therm. Anal. Calorim.* 47 (1996) 123–134.
- [45] I. Hamerton, A.M. Emsley, B.J. Howlin, P. Klewpatinond, S. Takeda, Studies on a dicyanate containing four phenylene rings and polycyanurate copolymers. 3. Application of mathematical models to determine the kinetics of the thermal degradation processes, *Polymer* 45 (2004) 2193–2199.
- [46] C. Di Blasi, C. Branca, A. Galgano, R. Moricone, E. Milella, Oxidation of a carbon/glass reinforced cyanate ester composite, *Polym. Degrad. Stabil.* 94 (2009) 1962–1971.
- [47] V.V. Korshak, S.-S.A. Pavlova, P.N. Gribkova, M.V. Tsirgiladze, V.A. Pankratov, S.V. Vinogradova, The mechanism of thermal and thermal-oxidative degradation of polymers containing s-triazine rings, *Polym. Sci. (USSR)* 22 (1980) 1875–1885.
- [48] C.P. Reghunadhan Nair, D. Mathew, K.N. Ninan, Imido-phenolic-triazine network polymers derived from maleimide-functional novolac, *Eur. Polym. J.* 37 (2001) 315–321.
- [49] D. Klinar, J. Golob, M. Krajnc, Curing of the diethylene glycol bis(allyl carbonate) determination of the kinetic triplet $A, E_{a,app}, f(\alpha)$ using the isoconversional method and compensation effect, *Chem. Biochem. Eng. Q.* 18 (2004) 65–71.
- [50] R.M.J. Westerhout, J. Waanders, J.A.M. Kuipers, W.P.M. Van Swaaij, Kinetics of the low-temperature pyrolysis of polyethylene, polypropene, and polystyrene modeling, experimental, determination, and comparison with literature models and data, *Ind. Eng. Chem. Res.* 36 (1997) 1955–1964.
- [51] H.H.G. Jellinek, *Aspects of Degradation and Stabilization of Polymers*, first ed., Elsevier, Amsterdam, 1978.
- [52] A.K. Burnham, L.N. Dinh, A comparison of isoconversional and model-fitting approaches to kinetic parameter estimation and application predictions, *J. Therm. Anal. Calorim.* 89 (2007) 479–490.
- [53] S. Vyazovkin, D. Dollimore, Linear and nonlinear procedures in isoconversional computations of the activation energy of nonisothermal reactions in solids, *J. Chem. Inf. Model.* 36 (1996) 42–45.
- [54] S. Vyazovkin, Evaluation of activation energy of thermally stimulated solid-state reactions under arbitrary variation of temperature, *J. Comput. Chem.* 18 (1997) 393–402.
- [55] S. Vyazovkin, Modification of the integral isoconversional method to account for variation in the activation energy, *J. Comput. Chem.* 22 (2001) 178–183.
- [56] Q.I. Rahman, G. Schmeisser, Characterization of the speed of convergence of the trapezoidal rule, *Numer. Mathem.* 57 (1990) 123–138.
- [57] S. Vyazovkin, N. Sbirrazzuoli, Kinetic analysis of isothermal cures performed below the limiting glass transition temperature, *Macromol. Rapid Commun.* 21 (2000) 85–90.
- [58] X.-G. Li, M.-R. Huang, Thermal decomposition kinetics of thermotropic poly(oxybenzoate-co-oxynaphthoate) Vectra copolyester, *Polym. Degrad. Stabil.* 64 (1999) 81–90.
- [59] M.-R. Huang, X.-G. Li, Thermal degradation of cellulose and cellulose esters, *J. Appl. Polym. Sci.* 68 (1998) 293–304.